

Multivalent Carbohydrate Recognition on a Glycodendrimer-Functionalized Flow-Through Chip

Hilbert M. Branderhorst,^[a] Rob Ruijtenbeek,^[b] Rob M. J. Liskamp,^[a] and Roland J. Pieters*^[a]

Dendrimers were fitted out with up to eight mannose moieties by "click" chemistry. They were subsequently attached to aluminum oxide chips via a spacer that was linked to the dendrimer core; this resulted in a microarray of glycodendrimers. Binding of the glycodendrimers to the fluorescent lectins ConA and GNA was observable in real time. In a single experiment it was possible to observe the multivalency enhancement or cluster effect in the binding event. This effect was small for ConA, in agreement with

its widely spaced binding sites, whereas it was large for GNA, with its twelve much more closely spaced binding sites. The dendrimer-fitted chip represents a valuable screening tool for multivalency effects. Furthermore kinetic and thermodynamic data on binding events can be deduced. Inhibition experiments are also possible with the system as was shown for ConA with α -methyl mannose as the inhibitor.

Introduction

Carbohydrate recognition is increasingly believed to be a crucial event in many biological processes, including the development of diseases such as (avian) flu,^[1] AIDS,^[2] and cancer.^[3] Increasing the understanding of the language of the carbohydrate-mediated communication between cells and its preventing pathological consequences are important goals in science.^[4] For DNA^[5] and peptide/protein^[6] recognition studies, biochips have been developed that have greatly increased the efficiency of these investigations due to miniaturization and the high-throughput characteristics of such microarrays. To apply such biochips to studies in carbohydrate recognition is a logical progression, and increasingly papers are appearing that report the development and/or application of carbohydrate microarrays.^[7] Reports describe the selective detection of carbohydrate-binding proteins, mostly lectins, on chips of various designs.^[8] In general, carbohydrates bind only weakly to their complementary proteins. To achieve biologically relevant binding, multivalency is often involved in natural carbohydrate recognition processes.^[9] To effectively interfere with multivalent protein-carbohydrate interactions it was found that multivalent inhibitors can be much more potent than their monovalent counterparts. A multivalent display of synthetic carbohydrate ligands has proven to be an effective inhibitor design for blocking for example, lectins,^[10] AB₅ toxins,^[11] and bacteria.^[12] In these cases a chelation type of mechanism is the likely cause of the enhancements, which can be very large and exceed a factor of 10⁴–10⁵. Examples in which chelation cannot play a role for geometric reasons typically show more moderate enhancements of below a factor of 100, except when large extended arrays are used.^[13] Despite successes, many features of multivalent carbohydrate binding require further study, such as the degree to which multivalency effects vary with the architecture of the protein (complex) and that of the multivalent ligand.^[14] We here take a step in that direction by adding the efficiency of microarrays to the study of multivalent interac-

tions. The present system enables the systematic screening of carbohydrate-binding proteins and can rapidly determine if they favor a multivalent carbohydrate display and also to what extent. Furthermore, selected binding parameters, including kinetic rate constants, can be deduced from the obtained data due the ability to monitor the binding in real time.

In order to do so, a flow-through microarray technology was used that had multivalent ligands spotted onto aluminium oxide^[15] porous chips.^[16] The use of porous chips has several advantages. It allows the analyte solution to be pumped up and down in the chip material to avoid diffusion limitations. Furthermore the binding process of the fluorescent protein to the chip can be monitored in real time. This is in contrast to the use of conventional chips in which only an end-point determination is possible after all nonbound fluorescent material has been washed away. The real-time monitoring is possible because the liquid that contains the fluorescent components is pumped up and down through the microchannels, which are unique to this chip material, which is controlled by the air pressure below the chip. Periodic pictures are taken by a CCD camera when the fluid with the nonbound fluorescent components is temporarily positioned below the chip where it will not be pictured by the camera. In this way, only fluorescence that results from binding is detected. Another advantage of

[a] H. M. Branderhorst, Prof. Dr. R. M. J. Liskamp, Dr. R. J. Pieters
Department of Medicinal Chemistry and Chemical Biology,
Utrecht Institute for Pharmaceutical Sciences, Utrecht University
P.O. Box 80082, 3508 TB Utrecht (The Netherlands)
Fax: (+31) 30-2536655
E-mail: r.j.pieters@uu.nl

[b] Dr. R. Ruijtenbeek
Pamgene International B.V.
P.O. Box 1335, 5200 BJ, 's Hertogenbosch, (The Netherlands)
Fax: (+31) 73-6158081

 Supporting information for this article is available on the WWW under <http://www.chembiochem.org> or from the author.

the three-dimensional porous material is that its internal surface to which ligands can be attached is approximately 500-fold larger than for two-dimensional spots on a glass surface. This high loading capacity has advantages for detecting weak binding processes. Additionally it is advantageous for our purpose because it allows us to place the ligands far apart to avoid undesirable multivalency effects due to proteins that bridge between ligands, which would mask the intended multivalency effects in the binding to glycodendrimers. In our studies we coupled mono- to octavalent mannose ligands to the chip surface, and we observed binding of the fluorescently labeled lectins concanavalin A (ConA) from the Jack bean seeds and the *Galanthus nivalis* agglutinin (GNA) from the snowdrop bulb. Distinct multivalent binding of the higher generation mannose dendrimers towards the GNA lectin was observed.

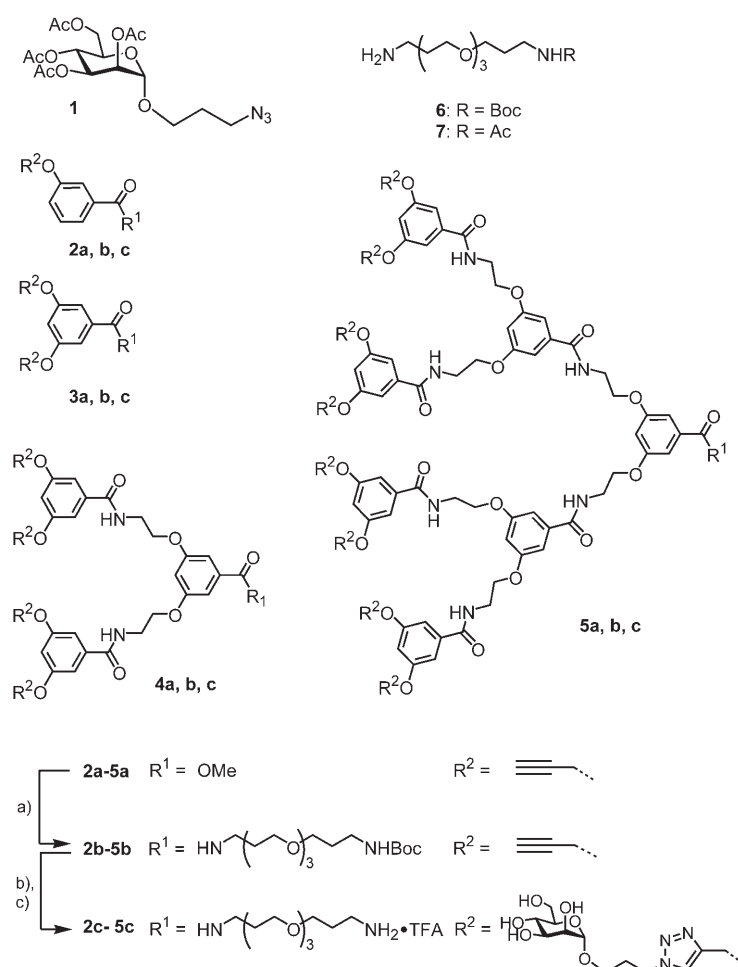
Results

In order to prepare the glycodendrimer chips, first dendrimers were prepared based on the 3,5-di-(2-aminoethoxy)-benzoic acid repeating unit.^[17] To attach the dendrimers to the chip surface, its core carboxylate was used for the attachment of a spacer. The spacer terminated in an amine; this allowed for conjugation at pH 9 to the chip-displayed maleimide function. The carbohydrates were attached to the dendrimer arm by “click” chemistry prior to attachment of the whole construct to the chip.^[18]

Synthesis of mannose dendrimers and attachment to the chip

Mannose azide building block **1**^[19] and alkyne-functionalized dendrimers **2a–5a**^[20] were prepared as previously reported (Scheme 1). Dendrimers **2a–5a** were treated with Tesser's base,^[21] followed by coupling to amine **6** with benzotriazole-1-yl-oxy-tris-(dimethylamino)-phosphonium hexafluorophosphate (BOP) as the coupling reagent. Decoration of the dendrimers with mannose moieties was achieved by using “click” chemistry under microwave irradiation, with copper(II) sulfate/sodium ascorbate as the copper(I) source.^[22] To this end, dendrimers **2b–5b** were treated with **1**. The obtained glycodendrimers were deacetylated by sodium methoxide, after which the *tert*-butoxycarbonyl (Boc) group was removed with trifluoroacetic acid (TFA). The pure **2c–5c** were obtained after preparative HPLC purification and were satisfactorily characterized by NMR spectroscopy and MS analysis.

Initial experiments on the chip were performed with dendrimers **2c–5c**, which reacted with the maleimide-functionalized chip surface at pH 9. The composition of the spotting solutions was chosen to have an equal mannose concentration in all solutions, despite the valency differences, that is, the dendrimer concentrations were corrected for their valency. We compared, for example, spots made from a 100 μM spotting



Scheme 1. Synthesis of dendrimers; reagents and conditions: a) i. NaOH, dioxane, MeOH, H₂O; ii. **6**, BOP, *i*Pr₂EtN, CH₂Cl₂/DMF, 40–95%; b) **1**, CuSO₄, sodium ascorbate, DMF, 80 °C, 20 min, 65–80%; c) i. NaOMe, MeOH, ii. TFA, H₂O, quantitative.

solution of monovalent **2c** to those made from a 12.5 μM spotting solution of octavalent **5c**, to yield chip surfaces as schematically shown in Figure 1. In a separate preparation we also corrected for the difference in amine concentrations of the spotting solutions by adding the nonsugar amine **7**, however this did not make a significant difference in the binding studies (see the Supporting Information) and was therefore not applied for the studies that are described below.

Binding experiments

The dendrimer solutions with varying concentrations and valencies were printed onto the microarray slides by using piezoelectric spotting of 330 pL per spot. A concentration range was applied from 0.1 to 5 mM mannose, and was corrected for the valency of the dendrimers, as mentioned before. Each array slide contained spots in quadruplicate. The experimental binding protocol started with the blocking of the nonfunctionalized area with BSA. A concentration range of FITC-labeled ConA was applied to the chips and the fluorescent signal was periodically recorded for 2 h (Figure 2), the fluorescent signal was quantified, averaged for the same spots, and converted to

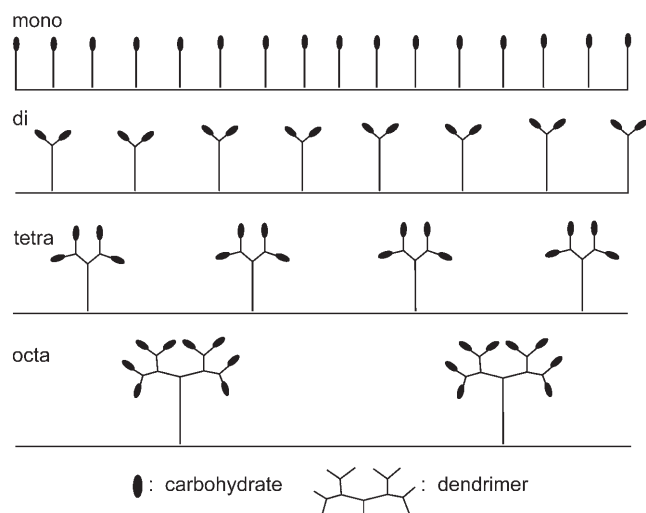


Figure 1. Microarray surfaces with identical mannose contents, but different valencies.

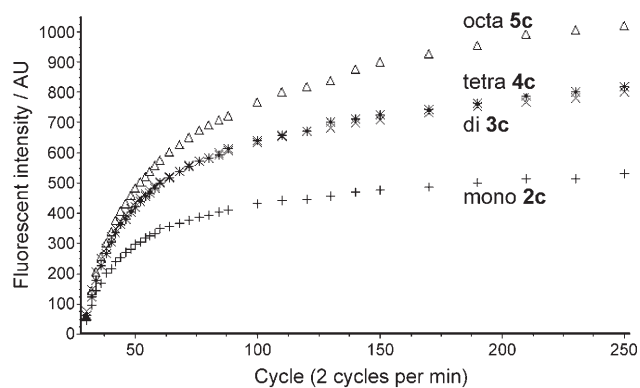


Figure 2. Progress curves for the microarray experiment with attached mono- to octavalent compounds **2c**–**5c** (spotting concentrations 0.5 mM in mannose) with a ConA (monomer concentration 98 nM).

progress curves. As a negative control, fluorescently labeled BS-I (*Bandeiraea simplicifolia* agglutinin) was used, which is specific for β -D-galactose residues. We did not observe any binding of this lectin towards the array surface. From the ConA results, we can clearly see the binding event of the lectin to the dendrimers as a function of time. It is also clear that the signal increases with the sugar density on the chip, which is a consequence of the more concentrated spotting solutions (Figure 3). A linear correlation between the spotting concentration and the observed equilibrium signal due to ConA binding was observed up to a 1 mM concentration of mannose residues (Supporting Information). This indicated that the concentrations of dendrimer-linked amine that were used were not enough to occupy all the maleimide sites. Furthermore, with the spotting concentration of 0.5 mM in mannose residues, as was used in the evaluations below, the calculated minimal intermolecular distance of the surface-bound ligands indicates that this is nonbridgeable by ConA.^[23] The multivalency effect that was observed for ConA was relatively small. The final equilibrium signals only varied by a factor of two, and favored the

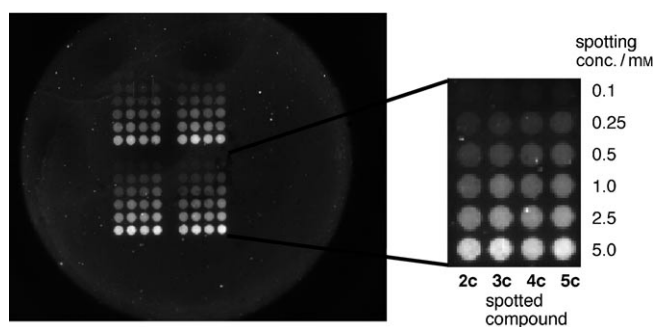


Figure 3. FITC-labeled ConA binds to the chip surface. In each of the four identical blocks the spotting concentration increases from top to bottom whereas the valency increases from left (mono **2c**) to right (octa **5c**).

octavalent presentation. Furthermore, the binding kinetics were similar for all compounds. By fitting the progress curves to a simple receptor–ligand interaction model, that is, a one-phase exponential association model, the observed rate constants of binding k_{obs} were obtained.^[24] These were all within the 0.20–0.23 min^{-1} range for the mono- to octavalent glyco-dendrimer-functionalized surfaces. Subsequently globally fitting the progress curves that were obtained from several ConA concentrations in the 0.2–1.0 μM range yielded the kinetic binding parameters k_{on} and k_{off} and the related kinetically determined dissociation constant K_{d} (Table 1) for each of the four

Table 1. Kinetic and thermodynamic parameters deduced from chip experiments for the association of ConA to the four different surfaces.

Compound on surface	k_{off} [$\text{M}^{-1} \text{min}^{-1}$] ^[a]	k_{on} [min^{-1}] ^[a]	K_{d} [nM] from binding kinetics ^[b]	equilibrium values ^[c]
mono 2c	0.12	1.26×10^5	950	960
di 3c	0.08	1.76×10^5	450	510
tetra 4c	0.07	1.76×10^5	400	540
octa 5c	0.04	1.93×10^5	210	440

[a] Derived from global fitting of progress curves for multiple conA concentrations. [b] $K_{\text{d}} = k_{\text{off}}/k_{\text{on}}$. [c] Derived from fitting end values by using different ConA concentrations to a Langmuir binding isotherm.

valencies. To see if reasonable numbers were obtained, the K_{d} 's were also determined by using equilibrium end values and a Langmuir binding isotherm. As can be seen in the table, the K_{d} values that were determined by these two methods were in the same range. The K_{d} for the octavalent **5c**-covered surface is the lowest, followed by tetra- and divalent **3c** and **4c**, which are very similar; the monovalent **2c**-covered surface interacted the weakest. The same trend can be seen from the progress curves in Figure 2; this illustrates the value of the technology as a rapid screening method to evaluate multivalency effects.

Subsequently, a higher-valency lectin, the *Galanthus nivalis* agglutinin (GNA) was studied. This lectin is tetrameric and has three binding sites per subunit, so twelve in total, and several of them are spaced closely together. The close spacing should allow chelation by the multivalent ligands, and thus strong

binding enhancement due to multivalency was expected. The monovalent affinity for mannose derivatives, however, is much lower: the K_d of α -methyl mannose for ConA is about $100 \mu\text{M}$,^[25] and for GNA this value is 24 mM .^[26] Despite the low affinity for mannose, binding was observable and indeed a strong preference for the higher-valency mannose dendrimers was observed (Figure 4). Furthermore the binding kinetics

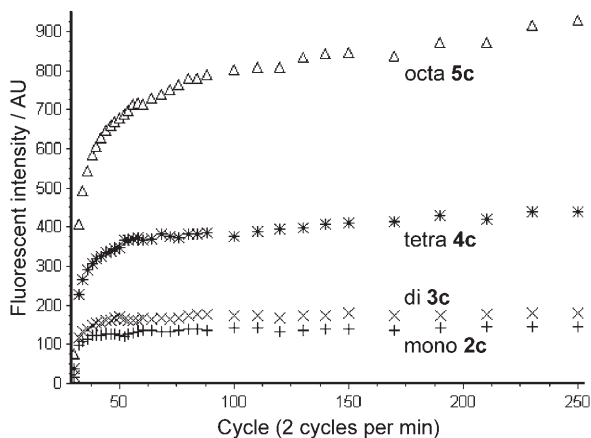


Figure 4. Progress curves for the microarray experiment with GNA (monomer concentration: $2 \mu\text{M}$). A clear preference for the higher-valency mannose dendrimers was observed.

were significantly faster than for the ConA experiment. It also appears that GNA binds slightly slower to the higher-valency compounds on the chip. The progress curves could not be fitted adequately to a one-phase exponential association model to obtain the k_{obs} . The use of a two-phase model was necessary, which yielded a low $k_{\text{obs}1}$ in the 0.03 – 0.08 min^{-1} range for all valencies, and also a faster $k_{\text{obs}2}$, which varied steadily with valency between 1.8 min^{-1} for the monovalent surface to 1.0 min^{-1} for the tetra- and octavalent compounds on the chip.

Inhibition experiment

The carbohydrate microarray system was also used for the evaluation of an inhibition experiment that was similar to those that were reported for other microarray systems.^[8b,27] To this end, the FITC-labeled ConA was incubated with the soluble inhibitor α -methyl mannose under several concentrations, and was added to spots of monovalent **2c**. A clear inhibition was observed that was used to determine an IC_{50} value of 400 (± 100) μM (Figure 5).

Discussion and Conclusion

Multivalent mannose dendrimers were prepared from alkyne dendrimers. The dendrimers were synthesized with an amine functional group linked to the dendrimeric core that allowed attachment to surfaces. The dendrimers that were based on the 3,5-di-(2-aminoethoxy)benzoic acid repeating unit were first equipped with a mono-Boc-protected diamino spacer

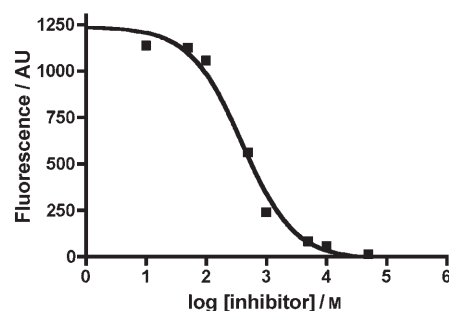


Figure 5. Inhibition data points and fitted curve of the binding of ConA to a chip of **2c** with increasing concentrations of α -methyl mannose in solution.

after which, the mannose residues were introduced at the periphery by the copper-catalyzed “click” reaction, and the compounds were fully deprotected. The mannose dendrimers were spotted onto a maleimide-functionalized porous aluminum oxide surface and binding of FITC-labeled lectins to the functionalized surfaces was clearly observed in real-time by using flow-through microarray technology. The flow-through microarray setup has several advantages over ordinary microarray technologies. Monitoring of progression of protein binding is important; not only endpoints, but also the binding kinetics were obtained. We demonstrated this technology for the binding of ConA and GNA towards multivalent compounds. Clear differences were seen in the responses of these proteins. ConA is a tetramer with binding sites that are separated by over 65 \AA , and are therefore too far apart to allow bridging by our dendrimers. No major multivalency effects were expected by our compounds, and indeed, they were not observed. In studies of related compounds, multivalency effects were limited to a factor of up to ~ 6 .^[28] Kinetic data were obtained from the chip experiments due to the possibility of real-time monitoring. By fitting a series of progress curves that were measured at different ConA concentrations, k_{on} and k_{off} values were obtained as well as the related kinetically determined dissociation constant K_d . The K_d was also determined by using the end points, and the numbers are of the same order of magnitude. The relative magnitude of the K_d values correlate well with the progress curves of the single experiment that is shown in Figure 2. This underscores the value of the present methodology as a screening tool that can rapidly identify multivalency effects, even in a single experimental run (and therefore well controlled). The magnitude of the K_d values was low (200 – 900 nM) in comparison to the reported K_d values of monovalent mannose derivatives that bind to conA, which are around $100 \mu\text{M}$.^[25,29] We speculate that the very long and very narrow pores of the aluminum oxide ($0.2 \mu\text{m}$ diameter, $60 \mu\text{m}$ height) are the cause. After dissociation, a rapid rebinding event is likely, which results in a net slow k_{off} . The determined k_{off} rate was seven-fold lower than that which was derived from using SPR methodology with immobilized yeast mannan,^[30] which is a system where k_{off} rates are likely already lowered due to the operative multivalency effects with the polymeric yeast mannan.

The phenomenon of enhanced binding due to the porous three-dimensional nature of the chip material is a bonus for the application of the technology as a screening tool for carbohydrate–protein interactions, which are typically weak. The combination that was used in this study of multivalency enhancement and the long pores make it possible to conveniently detect GNA binding, whose monovalent mannoside K_d is about 24 mM, by using only 2 μM of the protein (Figure 4). This results in low detection limits of weakly binding proteins. Whereas this study was not optimized for a low detection limit, by using a moderately dense substituted surface (spotting concentrations 0.5 mM in mannose) and an average shutter time of the CCD camera, ConA was detectable down to about 10 nM or 0.26 $\mu\text{g mL}^{-1}$. For comparison, the detection limit of an SPR-based system with immobilized yeast mannan was reported with a detection limit of 0.5 $\mu\text{g mL}^{-1}$ for ConA.^[30]

For GNA the effect of the multivalency was markedly different than for ConA. A strong signal for the immobilized octavalent compound **5c** was observed, and hardly any observable signal was seen for the mono- and divalent compounds (**2c–3c**) under the same conditions. This behavior is in-line with the high-valency architecture of the tetramer that is comprised of twelve binding sites in total with relatively closely spaced binding sites that start at around 20 Å, and the weak monovalent binding affinities in the millimolar range. Similar effects were also seen with the WGA lectin with eight binding sites and its binding to densely functionalized SPR chips.^[31] Based on our recent experiences with multivalent binding to cholera toxin, the spacers that were used here are too short for optimal multivalent binding.^[11f,32] Nevertheless strong multivalency was clearly observed.

The spotting concentrations that were used for the analysis of the ConA-binding parameters were in the range where the fluorescent signal still increases linearly with the spotting concentrations, that is, ≤ 1 mM in mannosides. For the GNA studies, a higher spotting concentration of 5.0 mM in mannosides was needed to get a strong enough signal, due to the weak inherent mannose affinity of this lectin. We cannot exclude that at this concentration the packing of the monovalent **2c** is sufficiently dense to allow bridging by GNA molecules, however considering the low signal of this binding event versus the GNA binding to the octavalent **5c**, which was spotted at only 0.625 mM, it seems highly unlikely.

In conclusion, the real-time evaluation of a multivalent carbohydrate chip as described here is a useful rapid screening method to evaluate multivalency effects in a single experiment. Extension of this study will be undertaken in the direction of other carbohydrates, other spacers, and other carbohydrate-binding proteins. Furthermore it is also clear that inhibition studies are also possible that provide additional potential for applications.

Experimental Section

General: Unless stated otherwise, chemicals were obtained from commercial sources and were used without further purification. Solvents were purchased from Biosolve (Valkenswaard, The Nether-

lands). Microwave reactions were carried out in a dedicated microwave oven, that is, the Biotage Initiator (Uppsala, Sweden). The microwave power was limited by temperature control once the desired temperature was reached. A sealed vessel of 2–5 mL was used. Analytical HPLC runs were performed on a Shimadzu automated HPLC system with a reversed-phase column (Alltech, Adsorbosphere C8, 90 Å, 5 μm , 250 \times 4.6 mm, Deerfield, IL, USA) that was equipped with an evaporative light-scattering detector (PL-ELS 1000, Polymer Laboratories, Amherst, MA, USA) and a UV/Vis detector that was operating at 220 and 254 nm. Preparative HPLC runs were performed on a Applied Biosystems workstation. Elution was effected by using a linear gradient of 5% MeCN/0.1% TFA in H₂O to 5% H₂O/0.1% TFA in MeCN. ¹H NMR (300 MHz) and ¹³C NMR (75.5 MHz) were performed on a Varian G-300 spectrometer.

Monovalent alkyne dendrimer (2b): A solution of **2a** (1.43 g, 7.5 mmol) was stirred in Tesser's base (50 mL) for 20 h. The mixture was acidified with aq KHSO₄ (1 M) to pH 2 and concentrated in vacuo. Crude product was taken up in EtOAc (100 mL) and washed twice with H₂O (50 mL) and with brine (50 mL). The organic phase was dried over Na₂SO₄, filtered and concentrated to give the free carboxylic acid (1.30 g, 98%). iPr₂EtN (0.99 mL, 6.0 mmol) was added to a solution of the acid (352 mg, 2.0 mmol), spacer **6** (0.96 g, 3.0 mmol), and BOP (1.33 g, 3.0 mmol) in CH₂Cl₂ (30 mL), and the reaction was stirred for 18 h. TLC (EtOAc) showed the formation of **2b**. The mixture was diluted with CH₂Cl₂ (100 mL), washed with 1 M KHSO₄ (50 mL), 5% NaHCO₃ (50 mL), and brine. The organic phase was dried over Na₂SO₄, filtered and concentrated. Silica column chromatography (EtOAc) afforded **2b** (775 mg, 81%). ¹H NMR (300 MHz, CDCl₃): δ = 7.45–7.29 (m, 3H; CH_{ar},2,5,6), 7.22 (brs, 1H; C(O)NH), 7.13 (brs, 1H; C(O)NH), 7.09 (dd, 1H; CH_{ar},4), 4.98 (brs, 1H; NHBoc), 4.73 (d, J = 2.4 Hz, 2H; OCH₂CCH), 3.66–3.45 (m, 14H; CH₂O, CH₂NHC(O)), 3.18 (q, 2H; CH₂NHBoc), 2.55 (t, J = 2.4 Hz, 1H; OCH₂CCH), 1.93–1.85 (m, 2H; OCH₂CH₂CH₂NH), 1.76–1.68 (m, 2H; OCH₂CH₂CH₂NH), 1.42 (s, 9H; NHC(O)OC(CH₃)₃); ¹³C NMR (75.5 MHz, CDCl₃): δ = 167.0 (C(O)NH), 157.6 (NHC(O)C(CH₃)₃), 157.6 (C_{ar},3), 136.2 (C_{ar},1), 129.4 (C_{ar},5), 119.8 (C_{ar},6), 118.1 (C_{ar},4), 113.5 (C_{ar},2), 79.0 (OCH₂CCH), 78.2 (NHC(O)C(CH₃)₃), 75.8 (OCH₂CCH), 70.2, 70.1, 70.0, 69.8, 69.2 (OCH₂), 55.9 (OCH₂CCH), 38.4 (CH₂NHBoc), 29.6, 28.8 (OCH₂CH₂CH₂NH), 28.3 (NHC(O)OC(CH₃)₃); HRMS calcd for C₂₅H₃₈N₂O₇ (478.2679): 501.262 [M+Na]⁺; found 501.240.

Divalent alkyne dendrimer (3b): A solution of **3a** (1.35 g, 5.53 mmol) was stirred in Tesser's base (75 mL) for 16 h. The mixture was acidified with aq 1 M KHSO₄ to pH 2 and concentrated in vacuo. Crude product was taken up in EtOAc (100 mL) and washed with 1 M KHSO₄ (50 mL), brine (50 mL) and H₂O (50 mL). The organic phase was dried over Na₂SO₄, filtered, and concentrated to give the free carboxylic acid (1.27 g, quantitative). iPr₂EtN (0.99 mL, 6.0 mmol) was added to a solution of the acid (460 mg, 2.0 mmol), spacer **6** (960 mg, 3.0 mmol), and BOP (1.33 g, 3.0 mmol) in CH₂Cl₂ (25 mL), and the solution was stirred for 2 h. TLC (CH₂Cl₂/MeOH, 19:1) showed full conversion. The mixture was diluted with CH₂Cl₂ (100 mL), washed with 1 M KHSO₄ (50 mL), 5% NaHCO₃ (50 mL), and brine (50 mL). The organic phase was dried over Na₂SO₄, filtered, and concentrated. Compound **3b** (1.10 g, quantitative) was isolated by silica column chromatography (CH₂Cl₂/MeOH, 19:1). ¹H NMR (300 MHz, CDCl₃): δ = 7.03 (brs, 3H; CH_{ar},2,6, NHC(O)), 6.73 (t, 1H; CH_{ar},4), 4.71 (d, 4H; 2OCH₂CCH, J = 2.2 Hz), 3.67–3.46 (m, 14H; CH₂O, CH₂NHC(O)), 3.18 (q, 2H; CH₂NHBoc), 2.55 (t, J = 2.2 Hz, 2H; OCH₂CCH), 1.93–1.85 (m, 2H; OCH₂CH₂CH₂NH), 1.76–1.68 (m, 2H; OCH₂CH₂CH₂NH), 1.41 (s, 9H; NHC(O)OC(CH₃)₃); ¹³C NMR

(75.5 MHz, CDCl₃): δ = 166.8 (C(O)NH), 156.2 (NHC(O)OC(CH₃)₃), 158.6 (C_{ar}3,5), 137.0 (C_{ar}1), 106.7 (C_{ar}2,6), 105.2 (C_{ar}4), 79.2 (OCH₂CCH), 78.1 (NHC(O)OC(CH₃)₃), 75.9 (OCH₂CCH), 70.2, 70.0, 69.9, 69.2 (OCH₂), 56.1 (OCH₂CCH), 38.5 (CH₂NHBoc), 29.6, 28.8 (OCH₂CH₂CH₂NH), 28.4 (NH(CO)OC(CH₃)₃); HRMS calcd for C₂₈H₄₀N₂O₈ 533.286 [M+H]⁺; found: 533.108.

Tetravalent alkyne dendrimer (4b): A solution of **4a** (680 mg, 1.0 mmol) was stirred in Tesser's base (30 mL) for 3 h. The mixture was acidified with aq 1 M KHSO₄ to pH 2 and concentrated in vacuo. Crude product was taken up in EtOAc (100 mL, with 10 mL of DMF) and washed twice with H₂O (50 mL) and brine (50 mL). The organic phase was dried over Na₂SO₄, filtered, and concentrated to give the free carboxylic acid (682 mg, quantitative). iPr₂EtN (0.50 mL, 3.0 mmol) was added to a solution of the acid (680 mg, 1.0 mmol), spacer **6** (480 mg, 1.5 mmol) and BOP (660 mg, 1.5 mmol) in DMF (40 mL), and the solution was stirred for 3 h. The mixture was concentrated in vacuo at 60 °C, and pure product was obtained after silica column chromatography (EtOAc/MeOH, 1:0→19:1) as a white foam (385 mg, 40%). ¹H NMR (300 MHz, DMSO): δ = 8.66 (t, 2H; C(O)NH), 8.41 (t, 1H; C(O)NH), 7.12 (s, 4H; CH_{ar}2',6'), 7.04 (s, 2H; CH_{ar}2,6), 6.78 (s, 2H; CH_{ar}4'), 6.73 (brs, 1H; NHBoc), 6.70 (s, 1H; CH_{ar}4), 4.83 (d, *J* = 2.4 Hz, 8H; OCH₂CCH), 4.15 (t, 4H; OCH₂CH₂N), 3.63 (q, 4H; OCH₂CH₂N), 3.57 (t, 2H; CH₂NHC(O)), 3.50–3.27 (m, 16H; CH₂O, CH₂NHC(O)), 2.93 (q, 2H; CH₂NHBoc), 2.50 (t, *J* = 1.8 Hz, 4H; OCH₂CCH), 1.78–1.70 (m, 2H; OCH₂CH₂CH₂NH), 1.62–1.54 (m, 2H; OCH₂CH₂CH₂NH), 1.36 (s, 9H; NHC(O)OC(CH₃)₃); ¹³C NMR (75.5 MHz, DMSO): δ = 165.7, 165.5 (C(O)NH), 159.4 (C_{ar}3,5), 158.1 (C_{ar}3',5'), 155.5 (NHC(O)OC(CH₃)₃), 136.7 (C_{ar}1), 36.3 (C_{ar}1'), 106.7(C_{ar}2',6'), 105.9 (C_{ar}2,6), 105.0 (C_{ar}4'), 103.8 (C_{ar}4), 78.9 (OCH₂CCH), 78.4 (OCH₂CCH), 77.4 (NHC(O)OC(CH₃)₃), 69.7, 69.5, 69.5, 68.2, 68.0, 66.2 (OCH₂), 55.8 (OCH₂CCH), 37.2 (CH₂NHC(O)), 36.6 (CH₂NHBoc), 29.7, 29.3 (OCH₂CH₂CH₂NH), 28.2 (NHC(O)OC(CH₃)₃); HRMS calcd for C₅₂H₆₂N₄O₁₄: 967.434 [M+H]⁺; found 967.096.

Octavalent alkyne dendrimer (5b): A solution of **5a** was stirred in Tesser's base. The mixture was acidified with aq 1 M KHSO₄ to pH 2 and concentrated in vacuo. Crude product was taken up in EtOAc (with 10% of DMF) and washed twice with H₂O (50 mL) and brine (50 mL). The organic phase was dried over Na₂SO₄, filtered, and concentrated to give the free carboxylic acid (quantitative). iPr₂EtN (248 μ L, 1.5 mmol) was added to a solution of the acid (767 mg, 0.5 mmol), spacer **6** (240 mg, 0.75 mmol) and BOP (332 mg, 0.75 mmol) in DMF (40 mL), and the solution was stirred for 20 h. The mixture was concentrated in vacuo at 60 °C, then taken up in EtOAc (100 mL), washed with 1 M KHSO₄ (50 mL), 5% NaHCO₃ (50 mL) and brine. The organic phase was dried over Na₂SO₄, filtered and concentrated. Silica column chromatography could not be used for purification because of solubility problems. The product was obtained after precipitation and centrifugation from DMF and EtOAc (1.55 g, 55%). ¹H NMR (300 MHz, DMSO): δ = 8.67 (brt, 6H; C(O)NH), 8.41 (t, 1H; C(O)NH), 7.13 (d, 8H; CH_{ar}2',6'), 7.08 (d, 4H; CH_{ar}2',6'), 7.03 (s, 2H; CH_{ar}2,6), 6.79 (d, 8H; CH_{ar}4'), 6.72 (s, 2H; CH_{ar}4'), 6.68 (s, 1H; CH_{ar}4), 4.83 (d, *J* = 1.9 Hz, 16H; OCH₂CCH), 4.14 (t, 12H; OCH₂CH₂N), 3.64–3.27 (m, 26H; CH₂O, CH₂NHC(O), OCH₂CH₂N), 2.95 (q, 2H; CH₂NHBoc), 2.50 (t, *J* = 1.7 Hz, 8H; OCH₂CCH), 1.77–1.69 (m, 2H; OCH₂CH₂CH₂NH), 1.62–1.54 (m, 2H; OCH₂CH₂CH₂NH), 1.36 (s, 9H; NHC(O)OC(CH₃)₃); ¹³C NMR (75.5 MHz, DMSO): δ = 165.5, 165.8, 165.9 (C(O)NH), 159.5 (C_{ar}3,5), 159.4 (C_{ar}3',5'), 158.2 (C_{ar}3',5'), 136.7 (C_{ar}1'), 136.3 (C_{ar}1'), 106.8(C_{ar}2',6'), 106.0 (C_{ar}2',5'), 105.0 (C_{ar}4'), 104.1 (C_{ar}4'), 78.9 (OCH₂CCH), 78.4 (OCH₂CCH), 69.7, 69.6, 68.2, 68.1, 66.2 (OCH₂), 55.8 (OCH₂CCH), 36.7

(CH₂NHBoc), 29.7, 29.3 (OCH₂CH₂CH₂NH), 28.2 (NHC(O)OC(CH₃)₃); HRMS calcd for C₁₀₀H₁₀₆N₆O₂₆: 1835.257 [M+H]⁺; found: 1835.730.

General "click" conditions: Alkyne dendrimer, sugar azide (1.5 equiv/alkyne), CuSO₄ (0.15 equiv/alkyne) and sodium ascorbate (0.3 equiv/alkyne) were dissolved in an appropriate volume of 1% H₂O in DMF. The mixture was heated under microwave irradiation to 80 °C for 20 min. The mixture was concentrated in vacuo at 60 °C, and the product was isolated by silica gel chromatography.

General deprotection procedure: Dendrimers were dissolved in MeOH. Catalytic NaOMe was added, and the reaction was stirred until TLC showed full deacetylation. The mixture was neutralized with Dowex H⁺, filtered, and concentrated in vacuo. The residue was stirred in 5% H₂O in TFA for 1 h. Solvents were evaporated and the product was purified by preparative HPLC and lyophilized from H₂O/MeCN.

Monovalent mannose dendrimer (2c): "Click" reaction was performed by the general procedure. Protected monovalent mannose dendrimer was isolated by silica gel chromatography (EtOAc/MeOH, 1:0→9:1) (147 mg, 81%). ¹H NMR (300 MHz, CDCl₃): δ = 7.64 (s, 1H; CH_{triazole}), 7.21–7.42 (m, 3H; CH_{ar}2,5,6), 7.15 (brs, 1H; C(O)NH), 7.02 (d, 1H; CH_{ar}4), 5.17–5.23 (m, 5H; H₂, H₃, H₄, OCH₂C_{triazole}), 4.95 (brs, 1H; NHBoc), 4.73 (s, 1H; H₁), 4.47–4.41 (m, 2H; CH₂O_{man}), 4.22 (dd, *J*_{5,6a} = 5.2 Hz, *J*_{6a,6b} = 12.1 Hz, 1H; H_{6a}), 4.02 (dd, *J*_{5,6b} = 2.5 Hz, *J*_{6a,6b} = 12.4 Hz, 1H; H_{6b}), 3.93–3.89 (m, 1H; H₅), 3.71–3.65 (m, 2H; CH₂NH(CO)), 3.59–3.35 (m, 12H; CH₂O), 3.14–3.08 (m, 2H; CH₂NHBoc), 2.21–2.12 (m, 2H; OCH₂CH₂CH₂N_{triazole}), 2.09 (s, 3H; C(O)CH₃), 2.01 (s, 3H; C(O)CH₃), 1.98 (s, 3H; C(O)CH₃), 1.92 (s, 3H; C(O)CH₃), 1.86–1.79 (m, 2H; OCH₂CH₂CH₂NH), 1.68–1.60 (m, 2H; OCH₂CH₂CH₂NH), 1.35 (s, 9H; NHC(O)OC(CH₃)₃); ¹³C NMR (75.5 MHz, CDCl₃): δ = 170.5, 170.0, 169.9, 169.6 (C(O)CH₃), 166.9 (C(O)NH), 156.0 (NHC(O)C(CH₃)₃), 158.2 (C_{ar}3), 143.7 (C_{triazole}4), 136.2 (C_{ar}1), 129.4 (C_{ar}5), 123.1 (C_{triazole}5), 119.3 (C_{ar}6), 117.8 (C_{ar}4), 113.4 (C_{ar}2), 97.6 (C₁), 70.3, 70.1, 70.0 and 69.3 (OCH₂), 69.3, 68.9, 68.6, 65.9, 64.5 (C₂, C₃, C₄, C₅, C₆), 62.3 (CH₂O_{man}), 61.8 (OCH₂C_{triazole}), 47.0 (CH₂N_{triazole}), 38.6 (CH₂NHBoc), 29.7 29.5, 28.8, (OCH₂CH₂CH₂NH, OCH₂CH₂CH₂N_{triazole}), 28.3 (NHC(O)OC(CH₃)₃), 20.7, 20.6, 20.5 (C(O)CH₃); HRMS calcd for C₄₂H₆₃N₅O₁₇: 932.4117 [M+Na]⁺; found: 932.3491. The dendrimer was deprotected according to the general deprotection procedure. Compound **2c** was isolated as a clear oil (54 mg, 88%). ¹H NMR (300 MHz, D₂O): δ = 8.10 (s, 1H; CH_{triazole}), 7.47–7.34 (s, 3H; CH_{ar}2,5,6), 7.23 (s, 1H; CH_{ar}4), 5.26 (s, 2H; OCH₂C_{triazole}), 4.71 (s, 1H; H₁), 4.53 (t, 2H; OCH₂CH₂NH), 3.81–3.40 (m, 24H; H₂, H₃, H₄, H₅, H₆, OCH₂, CH₂NH, CH₂N_{triazole}), 3.08 (t, 2H; CH₂NH₃), 2.23–2.15 (m, 2H; CH₂CH₂O_{Man}), 1.96–1.84 (m, 4H; OCH₂CH₂CH₂NH, OCH₂CH₂CH₂NH); ¹³C NMR (75.5 MHz, D₂O): δ = 170.5 (C(O)NH), 158.2 (C_{ar}3), 143.7 (C_{triazole}4), 136.0 (C_{ar}1), 130.9 (C_{ar}5), 125.9 (C_{triazole}5), 121.0 (C_{ar}6), 119.4 (C_{ar}4), 114.6 (C_{ar}2), 100.5 (C₁), 73.3, 71.2, 70.7, 67.3 (C₂, C₃, C₄, C₅), 70.3, 70.2, 70.0, 69.4, 68.9 (OCH₂), 65.0 (OCH₂C_{triazole}), 61.9 (OCH₂CH₂NH), 61.5 (C₆), 48.5 (CH₂N_{triazole}), 38.3, 38.0 (OCH₂CH₂NH, OCH₂CH₂CH₂NH), 29.7, 28.9, 27.1 (CH₂CH₂O_{Man}, OCH₂CH₂CH₂NH); HRMS calcd for C₂₉H₄₇N₅O₁₁: 642.7178 [M+H]⁺; found: 642.070.

Divalent mannose dendrimer (3c): "Click" reaction was performed by the general procedure. Protected divalent mannose dendrimer was isolated by silica gel chromatography (EtOAc/MeOH, 1:0→9:1) (210 mg, 75%). ¹H NMR (300 MHz, CDCl₃): δ = 7.65 (s, 2H; CH_{triazole}), 7.10 (brs, 1H; C(O)NH), 6.98 (d, 2H; CH_{ar}2,6), 6.69 (t, 1H; CH_{ar}4), 5.24–5.13 (m, 6H; H₂, H₃, H₄), 4.99 (brs, 1H; NHBoc), 4.73 (s, 2H; H₁), 4.48–4.39 (m, 4H; CH₂C_{triazole}), 4.22 (dd, *J*_{5,6a} = 5.2 Hz, *J*_{6a,6b} = 12.4 Hz, 1H; H_{6a}), 4.02 (dd, *J*_{5,6b} = 2.2 Hz, *J*_{6a,6b} = 12.4 Hz, 1H; H_{6b}), 3.91–3.87 (m, 2H; H₅), 3.71–3.66 (m, 2H; CH₂NHC(O)), 3.57–3.36 (m,

12H; CH₂O), 3.13–3.07 (m, 2H; CH₂NHBoc), 2.20–2.16 (m, 4H; OCH₂CH₂CH₂N_{triazole}), 2.09 (s, 3H; C(O)CH₃), 2.01 (s, 3H; C(O)CH₃), 1.97 (s, 3H; C(O)CH₃), 1.93 (s, 3H; C(O)CH₃), 1.86–1.78 (m, 2H; OCH₂CH₂CH₂NH), 1.65–1.61 (m, 2H; OCH₂CH₂CH₂NH), 1.35 (s, 9H; NHC(O)OC(CH₃)₃); ¹³C NMR (75.5 MHz, CDCl₃): δ = 170.5, 169.9, 169.8, 169.6 (C(O)CH₃), 166.7 (C(O)NH), 155.9 (NHC(O)C(CH₃)₃), 159.3 (C_{ar}3,5), 143.5 (C_{triazole}4), 137.1 (C_{ar}1), 123.1 (C_{triazole}5), 106.3 (C_{ar}2,6), 104.6 (C_{ar}4), 97.6 (C1), 70.3, 70.1, 70.0, 69.3 (OCH₂), 69.2, 68.9, 68.6, 65.9, 64.5 (C2, C3, C4, C5, C6), 62.3 (CH₂O_{man}), 61.9 (OCH₂C_{triazole}), 47.0 (CH₂N_{triazole}), 38.4 (CH₂NHBoc), 29.7, 29.5 and 28.8 (OCH₂CH₂CH₂NH, OCH₂CH₂CH₂N_{triazole}), 28.3 (NHC(O)OC(CH₃)₃), 20.7, 20.6, 20.5 (C(O)CH₃); HRMS calcd for C₆₂H₉₀N₈O₂₈: 1417.5763 [M+Na]⁺; found: 1417.7437. The dendrimer was deprotected according to the general deprotection procedure. Compound **3c** was isolated as a clear oil (70 mg, 91%). ¹H NMR (300 MHz, D₂O): δ = 8.06 (s, 2H; CH_{triazole}), 6.96 (s, 2H; CH_{ar}2,6), 6.76 (s, 1H; CH_{ar}4), 5.16 (s, 4H; OCH₂C_{triazole}), 4.70 (s, 2H; H1), 4.50 (t, 4H; OCH₂CH₂NH), 3.80–3.55 (m, 28H; H2, H3, H4, H5, H6, OCH₂), 3.50 (brs, 2H; CH₂NH), 3.40 (t, 4H; CH₂N_{triazole}), 3.07 (t, 2H; CH₂NH₃), 2.16 (t, 4H; CH₂CH₂O_{Man}), 1.94–1.83 (m, 4H; OCH₂CH₂CH₂NH, OCH₂CH₂CH₂NH); ¹³C NMR (75.5 MHz, D₂O): δ = 169.7 (C(O)NH), 159.5 (C_{ar}3,5), 143.6 (C_{triazole}), 136.9 (C_{ar}1), 125.9 (CH_{triazole}), 107.8 (C_{ar}2,6), 106.4 (C_{ar}4), 100.5 (C1), 73.4, 71.3, 70.7, 67.3 (C2, C3, C4, C5), 70.2 (OCH₂), 70.1 (OCH₂), 69.6 (OCH₂), 69.0 (OCH₂), 65.0 (OCH₂C_{triazole}), 62.0 (CH₂O_{Man}), 61.5 (C6), 48.5 (CH₂N_{triazole}), 38.3, 38.0 (OCH₂CH₂NH, OCH₂CH₂CH₂NH), 29.8, 29.0, 27.2 (CH₂CH₂O_{Man}, OCH₂CH₂CH₂NH); HRMS calcd for C₄₁H₆₆N₈O₁₈: 960.0129 [M+H]⁺; found: 959.188.

Tetraivalent mannose dendrimer (4c): “Click” reaction was performed by the general procedure. Protected tetraivalent mannose dendrimer was isolated by silica gel chromatography (CH₂Cl₂/MeOH, 9:1–4:1) as a white foam (163 mg, 59%). ¹H NMR (300 MHz, CDCl₃): δ = 7.76 (s, 4H; CH_{triazole}), 7.45 (s, 2H; C(O)NH), 7.36 (s, 1H; C(O)NH), 7.07 (s, 4H; CH_{ar}2,6), 6.94 (s, 2H; CH_{ar}2,6), 6.72 (s, 2H; CH_{ar}4), 6.59 (s, 1H; CH_{ar}4), 5.32–5.15 (m, 12H; H2, H3, H4), 4.80 (s, 4H; 4H1), 4.54–4.48 (m, 8H; CH₂O_{man}), 4.29 (dd, J_{5,6a} = 5.4 Hz, J_{6a,6b} = 12.3 Hz 1H; H6a), 4.08 (dd, J_{5,6b} = 2.4 Hz, J_{6a,6b} = 12.3 Hz, 1H; H6b), 3.96–4.00 (m, 4H; H5), 3.80–3.73 (m, 8H; CH₂N_{triazole}), 3.60–3.41 (m, 14H; CH₂O, CH₂NHC(O)), 3.18–3.12 (m, 2H; CH₂NHBoc), 2.29–2.19 (m, 8H; OCH₂CH₂CH₂N_{triazole}), 2.15 (s, 3H; C(O)CH₃), 2.08 (s, 3H; C(O)CH₃), 2.04 (s, 3H; C(O)CH₃), 1.99 (s, 3H; C(O)CH₃), 1.90–1.82 (m, 2H; OCH₂CH₂CH₂NH), 1.72–1.64 (m, 2H; OCH₂CH₂CH₂NH), 1.40 (s, 9H; NHC(O)OC(CH₃)₃); ¹³C NMR (75.5 MHz, CDCl₃): δ = 170.5, 169.9, 169.8, 169.5 (C(O)CH₃), 167.1, 166.7 (C(O)NH), 159.5 (C_{ar}3,5), 159.2 (C_{ar}3,5), 155.9 (NHC(O)C(CH₃)₃), 143.4 (C_{triazole}4), 136.9 (C_{ar}1), 136.4 (C_{ar}1), 123.3 (C_{triazole}5), 106.3 (C_{ar}2,6), 106.0 (C_{ar}2,6), 104.9 (C_{ar}4), 104.1 (C_{ar}4), 97.5 (C1), 78.7 (NHC(O)C(CH₃)₃), 70.1, 70.0, 69.8, 69.8 (OCH₂), 69.2, 68.9, 68.5, 65.8, 64.5 (C2, C3, C4, C5, C6), 62.2 (CH₂O_{man}), 61.7 (OCH₂C_{triazole}), 47.1 (CH₂N_{triazole}), 29.6, 29.4, 28.8 (OCH₂CH₂CH₂NH, OCH₂CH₂CH₂N_{triazole}), 28.2 (NHC(O)OC(CH₃)₃), 20.7, 20.6, 20.5 (C(O)CH₃); HRMS calcd for C₁₂₀H₁₆₂N₁₆O₅₄: 2714.0320 [M+Na]⁺; found 2714.3508. The dendrimer was deprotected according to the general deprotection procedure. Compound **4c** was isolated as a white powder (59 mg, quantitative). ¹H NMR (300 MHz, D₂O): δ = 7.91 (s, 4H; CH_{triazole}), 6.78 (s, 4H; CH_{ar}2,6), 6.76 (s, 2H; CH_{ar}2,6), 6.51 (s, 2H; CH_{ar}4), 6.39 (s, 1H; CH_{ar}4), 4.90 (s, 8H; OCH₂C_{triazole}), 4.69 (s, 4H; H1), 4.37 (brs, 8H; OCH₂CH₂NH), 3.96 (4H; bs, OCH₂CH₂NH), 3.81–3.46 (48H; m), 3.38–3.25 (8H; m, CH₂N_{triazole}), 3.08 (t, 2H; CH₂NH₃), 2.06 (8H; m, CH₂CH₂O_{Man}), 1.91 (q, 2H; OCH₂CH₂CH₂NH), 1.74 (brt, 2H; OCH₂CH₂CH₂NH); ¹³C NMR (75.5 MHz, D₂O): δ = 169.1 (C(O)NH), 160.0 (C_{ar}3,5), 159.4 (C_{ar}3,5), 143.5 (C_{triazole}4), 136.1 (C_{ar}1), 125.5 (C_{triazole}5), 107.2, 105.5 (C_{ar}), 100.4 (C1), 73.4, 71.3, 70.7, 67.3 (C2, C3, C4, C5), 70.1, 69.2, 68.9 (OCH₂), 64.8 (OCH₂C_{triazole}), 61.5 (C6), 48.4

(CH₂N_{triazole}), 38.3 (OCH₂CH₂NH), 29.9, 29.1, 27.1 (CH₂CH₂O_{Man}, OCH₂CH₂CH₂NH); HRMS calcd for C₈₃H₁₂₂N₁₆O₃₆ (1918.8208): 959.914 [M+2H]²⁺; found: 960.129

Octavalent mannose dendrimer (5c): A “click” reaction was performed by the general procedure. Protected octavalent mannose dendrimer was isolated by silica gel chromatography (CH₂Cl₂/MeOH, 1/0–9:1) (185 mg, 65%). ¹H NMR (300 MHz, CDCl₃): δ = 7.79 (brs, 8H; CH_{triazole}), 7.06 (brs, 8H; CH_{ar}2,6), 6.88 (brs, 6H; CH_{ar}2,6, 2,6), 6.67 (bs, 4H; CH_{ar}4), 6.44 (brs, 3H; CH_{ar}4, 4), 5.29–5.20 (m, 24H; H2, H3, H4), 4.80 (brs, 8H; H1), 4.50 (brs, 16H; CH₂O_{man}), 4.29 (brd, 8H; H6a), 4.07 (brd, 8H; H6b), 3.99 (brs, 8H; H5), 3.74 (brs, 16H; CH₂N_{triazole}), 3.59–3.47 (m, 14H; CH₂O, CH₂NHC(O)), 3.13 (brs, 2H; CH₂NHBoc), 2.23 (brs, 16H; OCH₂CH₂CH₂N_{triazole}), 2.15 (s, 24H; C(O)CH₃), 2.07 (s, 24H; C(O)CH₃), 2.04 (s, 24H; C(O)CH₃), 1.99 (s, 24H; C(O)CH₃), 1.90–1.82 (m, 2H; OCH₂CH₂CH₂NH), 1.72–1.64 (m, 2H; OCH₂CH₂CH₂NH), 1.39 (s, 9H; NHC(O)OC(CH₃)₃); ¹³C NMR (75.5 MHz, CDCl₃): δ = 170.3, 169.7, 169.6, 169.4 (C(O)CH₃), 167.1 (C(O)NH), 159.4 (C_{ar}3,5), 159.2 (C_{ar}3,5), 158.9 (C_{ar}3,5), 155.8 (NHC(O)C(CH₃)₃), 136.2 (C_{ar}1), 136.7 (C_{ar}1), 106.2 (C_{ar}2,6), 97.4 (C1), 78.5 (NHC(O)C(CH₃)₃), 70.2 (OCH₂), 69.0, 68.8, 68.3, 65.8, 64.5 (C2, C3, C4, C5, C6), 62.2 (CH₂O_{man}), 62.1 (OCH₂C_{triazole}), 47.8 (CH₂N_{triazole}), 29.5, 29.3, 28.3 (OCH₂CH₂CH₂NH, OCH₂CH₂CH₂N_{triazole}), 28.1 (NHC(O)OC(CH₃)₃), 20.5 (C(O)CH₃), 20.4 (C(O)CH₃); HRMS calcd for C₂₃₆H₃₀₆N₃₂O₁₀₆ (M, 5283.9538): 2666.543 [M+2Na]²⁺; found: 2666.540. A solution of 30% NaOMe in MeOH (50 μL) was added to a solution of the dendrimer (60 mg, 12 μmol) in MeOH (5 mL) and H₂O (5 mL) and stirred for 18 h. The reaction mixture was concentrated and taken up in H₂O (5 mL) and TFA (5 mL) was added. The reaction was stirred for 18 h, concentrated, and subjected to preparative HPLC purification. After lyophilization **5c** was obtained as white foam (40.2 mg, 92%). ¹H NMR (300 MHz, D₂O): δ = 7.88 (brs, 8H; CH_{triazole}), 6.79 (s, 8H; CH_{ar}2,6), 6.69 (s, 6H; CH_{ar}2,6, 2,6), 6.51 (s, 2H; CH_{ar}4), 6.27 (s, 2H; CH_{ar}4), 6.39 (s, 1H; CH_{ar}4), 4.87 (s, 16H; OCH₂C_{triazole}), 4.69 (s, 8H; H1), 4.34 (brs, 16H; OCH₂CH₂NH), 3.81–3.49 (100H; m), 3.31 (brs, 16H; CH₂N_{triazole}), 3.08 (t, 2H; CH₂NH₃), 2.02 (brs, 16H; CH₂CH₂O_{Man}), 1.95–1.91 (q, 2H; OCH₂CH₂CH₂NH); ¹³C NMR (75.5 MHz, D₂O): δ = 168.9 (C(O)NH), 159.9 (C_{ar}3,5), 159.4 (C_{ar}3,5), 143.4 (C_{triazole}4), 136.1 (C_{ar}1), 125.4 (C_{triazole}5), 107.1 (C_{ar}), 100.4 (C1), 73.4, 71.3, 70.7, 67.3 (C2, C3, C4, C5), 70.1 (OCH₂), 64.8 (OCH₂C_{triazole}), 61.5 (C6), 48.3 (CH₂N_{triazole}), 38.3 (OCH₂CH₂NH), 30.8 (CH₂CH₂O_{Man}, OCH₂CH₂CH₂NH). MALDI ToF HRMS calcd for C₁₆₇H₂₃₄N₃₂O₇₂ (M, 3841.8161): 3842.8235 [M+H]⁺; found: 3842.4735.

Microarray analysis: Microarray experiments were performed by using PamChip® arrays run on a PamStation®12 instrument (PamGene B.V., 's Hertogenbosch, The Netherlands). Temperature-controlled mannose chips were run in parallel by pumping the sample up and down through the 3-dimensional porous chip. Data were captured by real-time imaging of the fluorescence signal by CCD imaging. Images were analyzed by BioNavigator software (PamGene B.V., 's Hertogenbosch, The Netherlands). The fluorescent intensities were expressed as arbitrary units and the relative intensities of individual dendrimers was the average of four spots.

Detection of Dendrimer-ConA binding: A concentration range of FITC-labeled ConA (25–0.5 μg mL⁻¹) in HEPES/BSA buffer that contained Ca²⁺ and Mn²⁺ (10 mM HEPES, 1 mM CaCl₂, 1 mM MnCl₂, 100 mM NaCl, 0.1% BSA, pH 7.5) was used for binding experiments. Determination of the observed rate constant *k*_{obs} was performed by fitting the data to an exponential association equation, within GraphPad Prism v.4/5 the “one-phase exponential association” model was used. The kinetic parameters *k*_{on}, *k*_{off} and the related *K*_d were determined by a global fit of multiple binding progress

curves that were determined by different ConA concentrations, within GraphPad Prism v.4/5 the "Association kinetics—two or more conc. of hot." model was used, globally sharing the k_{on} , k_{off} and the B_{max} . The K_d that was based on equilibrium end-value was determined by fitting these values as a function of the ConA concentration by using the GraphPad Prism v.4/5 the "One-site binding (hyperbola)" model.

Detection of dendrimer-GNA binding: A concentration range of FITC-labeled GNA ($100\text{--}5\ \mu\text{g mL}^{-1}$) in HEPES/BSA buffer (10 mM HEPES, 100 mM NaCl, 0.1% BSA, pH 7.5) was used for binding experiments. Determination of the observed rate constant k_{obs} was performed by fitting the data to an exponential association equation, within GraphPad Prims v.4/5 the "Two-phase exponential association" model was used.

Negative control: A concentration range of FITC-labeled BS-I ($250\text{--}10\ \mu\text{g mL}^{-1}$) in HEPES/BSA buffer (10 mM HEPES, 100 mM NaCl, 0.1% BSA, pH 7.5) was used for binding experiments.

Acknowledgements

The Utrecht Institute for Pharmaceutical Sciences is gratefully acknowledged for support. We thank Ir. Iskandar Gandasmita for immobilizing the glycodendrimers on the chip by piezoelectric spotting and Dr. Nico de Mol for helpful discussion about the binding kinetics.

Keywords: carbohydrates • glycodendrimers • inhibitors • lectins • microarrays • multivalency

- [1] a) J. Stevens, O. Blixt, T. M. Tumpey, J. K. Taubenberger, J. C. Paulson, I. A. Wilson, *Science* **2006**, *312*, 404–410; b) M. J. Kiefel, M. von Itzstein, *Chem. Rev.* **2002**, *102*, 471–490.
- [2] L.-X. Wang, *Curr. Opin. Drug Discovery Dev.* **2006**, *9*, 194–206.
- [3] G. Ragupathi, F. Koide, P. O. Livingston, Y. S. Cho, A. Endo, Q. Wan, M. K. Spassova, S. J. Keding, J. Allen, O. Ouerfelli, R. M. Wilson, S. J. Danishefsky, *J. Am. Chem. Soc.* **2006**, *128*, 2715–2725.
- [4] a) D. B. Werz, P. H. Seeberger, *Chem. Eur. J.* **2005**, *11*, 3194–3206; b) K. J. Doores, D. P. Gamblin, B. G. Davis, *Chem. Eur. J.* **2006**, *12*, 656–666.
- [5] J. Khan, M. L. Bittner, Y. Chen, P. S. Meltzer, J. M. Trent, *Biochim. Biophys. Acta* **1999**, *1423*, M17–M28.
- [6] H. Zhu, M. Snyder, *Curr. Opin. Chem. Biol.* **2003**, *7*, 55–63.
- [7] a) J. L. de Paz, P. H. Seeberger, *QSAR Comb. Sci.* **2006**, *25*, 1027–1032; b) I. Shin, S. Park, M. Lee, *Chem. Eur. J.* **2005**, *11*, 2894–2901; c) J. C. Paulson, O. Blixt, B. E. Collins, *Nat. Chem. Biol.* **2006**, *2*, 238–248; d) D. Wang, *Proteomics* **2003**, *3*, 2167–2175; e) T. Feizi, F. Fazio, W. Chai, C.-H. Wong, *Curr. Opin. Struct. Biol.* **2003**, *13*, 637–645.
- [8] a) K. T. Pilobello, L. Krishnamoorthy, D. Slawek, L. K. Mahal, *ChemBioChem* **2005**, *6*, 985–989; b) J. C. Manimala, T. A. Roach, Z. Li, J. C. Gildersleeve, *Angew. Chem.* **2006**, *118*, 3689–3692; *Angew. Chem. Int. Ed.* **2006**, *45*, 3607–3610; c) K.-S. Ko, F. A. Jaipuri, N. L. Pohl, *J. Am. Chem. Soc.* **2005**, *127*, 13162–13163; d) B. T. Houseman, M. Mrksich, *Chem. Biol.* **2002**, *9*, 443–454; e) Z. Pei, H. Yu, M. Theurer, A. Waldén, P. Nilsson, M. Yan, O. Ramström, *ChemBioChem* **2007**, *8*, 166–168; f) J. L. de Paz, C. Noti, P. H. Seeberger, *J. Am. Chem. Soc.* **2006**, *128*, 2766–2767; g) E. W. Adams, D. M. Ratner, H. R. Bokesch, J. B. McMahon, B. R. O'Keefe, P. H. Seeberger, *Chem. Biol.* **2004**, *11*, 875–881; h) X.-L. Sun, C. L. Stabler, C. S. Cazalis, E. L. Chaikof, *Bioconjugate Chem.* **2006**, *17*, 52–57.
- [9] a) M. Mammen, S.-K. Chio, G. M. Whitesides, *Angew. Chem.* **1998**, *110*, 2908–2953; *Angew. Chem. Int. Ed.* **1998**, *37*, 2754–2794; b) L. L. Kiessling, L. E. Strong, J. E. Gestwicki, *Ann. Rep. Med. Chem.* **2000**, *35*, 321–330; c) T. K. Lindhorst, *Top. Curr. Chem.* **2002**, *218*, 201–235; d) R. T. Lee, Y. C. Lee, *Glycoconjugate J.* **2000**, *17*, 543–551; e) B. Turnbull, J. F. Stoddart, *Rev. Mol. Biotechnol.* **2002**, *90*, 231–255; f) M. J. Cloninger, *Curr. Opin. Chem. Biol.* **2002**, *6*, 742–748; g) R. Roy, *Trends Glycosci. Glycotechnol.* **2003**, *15*, 291–310; h) R. J. Pieters, *Trends Glycosci. Glycotechnol.* **2004**, *16*, 243–254.
- [10] a) R. T. Lee, Y. C. Lee, *Glycoconjugate J.* **2000**, *17*, 543; b) C. Maierhofer, K. Rohmer, V. Wittmann, *Bioorg. Med. Chem.* **2007**, *15*, 7661–7676.
- [11] a) J. P. Thompson, C.-L. Schengrund, *Glycoconjugate J.* **1997**, *14*, 837–845; b) Z. Zhang, E. A. Merritt, M. Ahn, C. Roach, Z. Hou, C. L. M. J. Verlinde, W. G. J. Hol, E. Fan, *J. Am. Chem. Soc.* **2002**, *124*, 12991–12998; c) D. Arosio, I. Vrasidas, P. Valentini, R. M. J. Liskamp, R. J. Pieters, A. Bernardi, *Org. Biomol. Chem.* **2004**, *2*, 2113–2124; d) Z. Zhang, J. C. Pickens, W. G. J. Hol, E. Fan, *Org. Lett.* **2004**, *6*, 1377–1380; e) P. I. Kitov, J. M. Sadowska, G. Mulvey, G. D. Armstrong, H. Ling, N. S. Pannu, R. J. Read, D. R. Bundle, *Nature* **2000**, *403*, 669–672; f) A. V. Pukin, H. M. Branderhorst, C. Sisu, C. A. G. M. Weijers, M. Gilbert, R. M. J. Liskamp, G. M. Visser, H. Zuilhof, R. J. Pieters, *ChemBioChem* **2007**, *8*, 1500–1503.
- [12] a) H. C. Hansen, S. Haataja, J. Finne, G. Magnusson, *J. Am. Chem. Soc.* **1997**, *119*, 6974–6979; b) R. Autar, A. S. Kahn, M. Schad, J. Hacker, R. M. J. Liskamp, R. J. Pieters, *ChemBioChem* **2003**, *4*, 1317–1325; c) J. A. F. Joosten, V. Loimaranta, C. C. M. Appeldoorn, S. Haataja, F. A. el Maate, R. M. J. Liskamp, J. Finne, R. J. Pieters, *J. Med. Chem.* **2004**, *47*, 6499–6508.
- [13] T. K. Dam, T. A. Gerken, B. S. Cavada, K. S. Nascimento, T. R. Moura, C. F. Brewer, *J. Biol. Chem.* **2007**, *282*, 28256–28263.
- [14] For activities in that direction see: a) J. E. Gestwicki, C. W. Cairo, L. E. Strong, K. A. Oetjen, L. L. Kiessling, *J. Am. Chem. Soc.* **2002**, *124*, 14922–14933; b) M. Gómez-García, J. M. Benito, D. Rodríguez-Lucena, J.-X. Yu, K. Chmurski, C. Ortiz Mellet, R. Gutiérrez Gallego, A. Maestre, J. Defaye, J. M. García Fernández, *J. Am. Chem. Soc.* **2005**, *127*, 7970–7971; c) M. L. Wolfenden, M. J. Cloninger, *Bioconjugate Chem.* **2006**, *17*, 958–966.
- [15] S. E. Jones, S. A. Ditner, C. Freeman, C. J. Whitaker, M. A. Lock, *Appl. Environ. Microbiol.* **1989**, *55*, 529–530.
- [16] a) R. van Beuningen, H. van Damme, P. J. Boender, N. Bastiaensen, A. B. Chan, T. Kievits, *Clin. Chem.* **2001**, *10*, 1931–1933; b) Y. Wu, P. de Kievit, L. Vahlkamp, D. Pijnenburg, M. Smit, M. Dankers, D. Melchers, M. Stax, P. J. Boender, C. Ingham, N. Bastiaensen, R. de Wijn, D. van Alewijk, H. van Damme, A. K. Raap, A. B. Chan, R. van Beuningen, *Nucleic Acids Res.* **2004**, *32*, e123; c) S. Lemeer, C. Jopling, F. Naji, R. Ruijtenbeek, M. Slijper, A. J. R. Heck, J. den Hartog, *PLoS ONE* **2007**, *2*, e581; d) S. Lemeer, R. Ruijtenbeek, M. W. Pinkse, C. Jopling, A. J. Heck, J. den Hertog, M. Slijper, *Mol. Cell Proteomics* **2007**, *6*, 2088–2099.
- [17] A. J. Brouwer, S. J. E. Mulders, R. M. J. Liskamp, *Eur. J. Org. Chem.* **2001**, 1903–1915.
- [18] a) V. V. Rostovtsev, L. G. Green, V. V. Fokin, K. B. Sharpless, *Angew. Chem.* **2002**, *114*, 2708–2711; *Angew. Chem. Int. Ed.* **2002**, *41*, 2596–2599; b) C. W. Tornøe, C. Christensen, M. Meldal, *J. Org. Chem.* **2002**, *67*, 3057–3064; c) C. M. Tornøe, M. Meldal, *Peptides: The Wave of the Future, Proceeding of the Second International and the Seventeenth American Peptide Symposium*, (Ed.: M. Lebl, R. A. Houghten), **2001**, pp. 263–264; d) P. Wu, V. V. Fokin, *Aldrichimica Acta* **2007**, *40*, 7–17; e) S. A. Nepogodiev, S. Dedola, L. Marmuse, M. T. de Oliveira, R. A. Field, *Carbohydr. Res.* **2007**, *342*, 529–540; f) S. G. Gouin, L. Bultel, C. Falentin, J. Kovensky, *Eur. J. Org. Chem.* **2007**, 1160–1167; g) S. G. Gouin, E. Vanquelf, J. M. García Fernández, C. Ortiz Mellet, F.-Y. Dupradeau, J. Kovensky, *J. Org. Chem.* **2007**, *72*, 9032–9045; h) R. J. Pieters, D. T. S. Rijkers, R. M. J. Liskamp, *QSAR Comb. Sci.* **2007**, *26*, 1181–1190.
- [19] C. C. M. Appeldoorn, J. A. F. Joosten, F. Ait el Maate, U. Dobrindt, J. Hacker, R. M. J. Liskamp, S. Kahn, R. J. Pieters, *Tetrahedron: Asymmetry* **2005**, *16*, 361–372.
- [20] D. T. S. Rijkers, G. W. van Esse, R. Merx, A. J. Brouwer, H. J. F. Jacobs, R. J. Pieters, R. M. J. Liskamp, *Chem. Commun. (Cambridge)* **2005**, 4581–4583.
- [21] Tesser's base is a mixture of dioxane, methanol and aqueous sodium hydroxide, see: G. I. Tesser, I. C. Balvert-Geers, *Int. J. Pept. Protein Res.* **1975**, *7*, 295.
- [22] J. A. F. Joosten, N. T. H. Tholen, F. Ait El Maate, A. J. Brouwer, G. W. van Esse, D. T. S. Rijkers, R. M. J. Liskamp, R. J. Pieters, *Eur. J. Org. Chem.* **2005**, 3182–3185.
- [23] The chip material has a surface increase (relative to a flat surface) of approx. 500-fold. The spots have a 60 μm radius. The number of maleimides can be considered non-limiting. If we assume a theoretical (and likely unrealistically high) 95% coupling efficiency to all available internal surface with 300 pL of the spotting solution, a 0.5 mM concentration of monovalent ligand concentration leads to an average interli-

- gand distance of 87 Å (see the Supporting Information for the calculation), and for the octavalent ligand (0.0625 mM) the distance is 247 Å. The ConA binding sites are spanned by a distance of about 70 Å.
- [24] The fits were adequate, although using a two-phase exponential improves the fit due to an additional parameter.
- [25] a) J. B. Corbell, J. L. Lundquist, E. J. Toone, *Tetrahedron: Asymmetry* **2000**, *11*, 95–111; b) T. K. Dam, R. Roy, S. K. Das, S. Oscarson, C. F. Brewer, *J. Biol. Chem.* **2000**, *275*, 14223–14230.
- [26] H. Kaku, I. J. Goldstein, *Carbohydr. Res.* **1992**, *229*, 337–346.
- [27] a) S. Park, M.-r Lee, S.-J. Pyo, I. Shin, *J. Am. Chem. Soc.* **2004**, *126*, 4812–4819; b) X. Zhou, J. Zhou, *Biosens. Bioelectron.* **2006**, *21*, 1451–1458; c) P.-H. Liang, S.-K. Wang, C.-H. Wong, *J. Am. Chem. Soc.* **2007**, *129*, 11177–11184; d) J. de Paz, C. Noti, F. Böhm, S. Werner, P. H. Seeberger, *Chem. Biol.* **2007**, *14*, 879–887.
- [28] a) M. Köhn, J. M. Benito, C. Ortiz Mellet, T. K. Lindhorst, J. M. García Fernández, *ChemBioChem* **2004**, *5*, 771–777; b) E. K. Woller, M. J. Cloninger, *Org. Lett.* **2002**, *4*, 7–10; c) T. K. Dam, R. Roy, S. K. Das, S. Oscarson, C. F. Brewer, *J. Biol. Chem.* **2000**, *275*, 14223–14230; d) D. Pagé, S. Aravind, R. Roy, *Chem. Commun.* **1996**, 1913–1914.
- [29] A low dissociation constant for ConA (180 nM) on densely mannose-functionalized SPR chips was previously measured, which was likely caused by multivalent binding, which, as discussed, is unlikely the case here; see: E. A. Smith, W. D. Thomas, L. L. Kiesling, R. M. Corn, *J. Am. Chem. Soc.* **2003**, *125*, 6140–6148.
- [30] W. Vornholt, M. Hartmann, M. Keusgen, *Biosens. Bioelectron.* **2007**, *22*, 2983–2988.
- [31] Y. Shinohara, Y. Hasegawa, H. Kaku, N. Shibuya, *Glycobiology* **1997**, *7*, 1201–1208.
- [32] H. M. Branderhorst, R. M. J. Liskamp, G. M. Visser, R. J. Pieters, *Chem. Commun. (Cambridge)* **2007**, 5043–5045.

Received: March 28, 2008

Published online on July 4, 2008